AWARD NUMBER: W81XWH-18-1-0517

TITLE: A Novel Ex Vivo Energy-Enhanced Hypothermic Preservation of Skin-Containing Composite Tissues

PRINCIPAL INVESTIGATOR: El Rasheid Zakaria

CONTRACTING ORGANIZATION: University of Arizona
Tucson, AZ 85719- 4824

REPORT DATE: Dec 2019

TYPE OF REPORT: Final

PREPARED FOR: U.S. Army Medical Research and Development Command
Fort Detrick, Maryland 21702-5012

REPORT DOCUMENTATION PAGE

Form Approved
OMB No. 0704-0188

1. REPORT DATE	2. REPORT TYPE	3. DATES COVERED
Dec 2019	Final	15 Aug 2018 – 14 Aug 2019

4. TITLE AND SUBTITLE

A Novel Ex Vivo Energy-Enhanced Hypothermic Preservation of Skin-Containing Composite Tissues

5a. CONTRACT NUMBER

5b. GRANT NUMBER
W81XWH-18-1-0517

5c. PROGRAM ELEMENT NUMBER

6. AUTHOR(S)

El Rasheid Zakaria

E-Mail: drelzak@surgery.arizona.edu

5d. PROJECT NUMBER

5e. TASK NUMBER

5f. WORK UNIT NUMBER

7. PERFORMING ORGANIZATION NAME(S) AND ADDRESS(ES)

University of Arizona
Arizona Board of Regents
888 N Euclid Ave. Rm 510
Tucson, AZ 85719- 4824

8. PERFORMING ORGANIZATION REPORT NUMBER

9. SPONSORING / MONITORING AGENCY NAME(S) AND ADDRESS(ES)

U.S. Army Medical Research and Development Command
Fort Detrick, Maryland 21702-5012

10. SPONSOR/MONITOR'S ACRONYM(S)

11. SPONSOR/MONITOR'S REPORT NUMBER(S)

12. DISTRIBUTION / AVAILABILITY STATEMENT

Approved for Public Release; Distribution Unlimited

13. SUPPLEMENTARY NOTES

14. ABSTRACT:

The overall objective of this project was to increase composite tissue tolerance to 24 hours of extended cold ischemia time. To achieve this, paired hindlimbs in rats were randomized to receive isolated hypothermic perfusions with either the University of Wisconsin (UW) solution (control), or the UW + ATPv solution (experimental). ATPv are nanoscale fusogenic lipid vesicles encapsulating ATP and capable of delivering ATP directly into the cytosol of cells. Upon completion of the perfusion, hindlimbs were conserved in static cold storage for either 12, 16 or 24 hours before skin and muscles were harvested for viability assessment. The extended cold ischemia times invariably degraded tissue nucleotides and countered the optimum temperature required for enzymatic actions. These effects rendered nucleotide- and enzyme-dependent tests of viability unreliable. Energy enhanced (ATPv) ex vivo hypothermic perfusions extended hindlimb composite tissue tolerance to 24h of cold ischemia without remarkable vascular or muscle damages. The vascular endothelium exhibited the least tolerance to cold ischemia relative to the skeletal muscle and skin. The addition of O_2 to the crystalloid perfusion solutions does not enhance composite tissue tolerance to cold ischemia. Linking the subcellular structural changes to the prevailing proteome provided the best muscle viability index after cold ischemia.

15. SUBJECT TERMS
Vascularized composite allotransplantation; Composite tissue; Lipid vesicles; Energy delivery vehicle; ATPv; Cytosolic energy; ATP; Tissue viability; Cold ischemia.

16. SECURITY CLASSIFICATION OF:			17. LIMITATION OF ABSTRACT	18. NUMBER OF PAGES	19a. NAME OF RESPONSIBLE PERSON
a. REPORT	b. ABSTRACT	c. THIS PAGE			USAMRMC
Unclassified	Unclassified	Unclassified	Unclassified	26	19b. TELEPHONE NUMBER *(include area code)*

Standard Form 298 (Rev. 8-98)
Prescribed by ANSI Std. Z39.18

TABLE OF CONTENTS

INTRODUCTION

Vascularized composite allotransplantation (VCA) is a restorative surgical procedure to treat whole or partly disfiguring craniofacial and extremity injuries. However, a limited availability and quality of donor allografts hampers the routine clinical use of VCA surgery. Face or upper extremity allografts for VCA surgery are essentially procured from a brain-dead donor and subsequently preserved in a hypothermic environment until their transplantation in a suitable recipient. Hypothermic allograft preservation whether by simple static cold storage or by hypothermic extracorporeal perfusion is intended to decrease the composite tissue metabolic demands and passively conserves energy. These preservation strategies are ineffective in creating a positive cellular energy balance to sustain the energy-dependent cellular processes and maintain composite tissue viability. The purpose of our project was to provide an alternative to the current passive cellular energy conservation strategies. Our novel strategy was based on actively replenishing the depleted cellular cytosolic energy stores. We achieved this strategy by using lipid vesicles encapsulating *adenosine-5` - triphosphate* (ATP). These cellular energy delivery vehicles (ATPv) are highly fusogenic phospholipid vesicles that ensure the direct replenishment of the cellular cytosolic ATP in concentrations exceeding the cellular metabolic demands. The scope of our research project was to demonstrate that in a rat model of bilateral hindlimb's randomized *ex vivo* perfusions, only the energy enhanced (ATPv) perfusate increases the hindlimb's composite tissue tolerance to static cold storage and extends the cold ischemia time up to 24 hours. Tolerance and composite tissue viability between the control and experimental hindlimbs were accessed by a composite index that measured tissue appearance, histology, total tissue water, and cytokine signatures.

KEYWORDS

Vascularized composite allotransplantation; Composite tissue; Lipid vesicles; Energy delivery vehicle; ATPv; Cytosolic energy; ATP; Tissue viability; Cold ischemia.

ACCOMPLISHMENTS

Our project was set to accomplish the following goals: 1) measuring the hindlimb tissue viability at 12, 16 or 24 hours of static cold storage after ipsilateral hypothermic perfusion with energy-enhanced University of Wisconsin (UW) perfusate (UW + ATPv), and contralateral hypothermic perfusion using the UW-perfusate as a control; and 2) measuring the hindlimb tissue vitality at 12, 16 or 24 hours of static cold storage after ipsilateral hypothermic perfusion with oxygen supplemented, energy-enhanced UW perfusate (UW + O_2 + ATPv); and contralateral hypothermic perfusion using oxygen supplemented UW-perfusate (UW + O_2) as a control. The major objective of our project was to enhance tolerance of the composite tissue of the hindlimb allograft to 24h of cold ischemia time after *ex vivo* perfusion. To fulfil this objective, we utilized an established rat model of isolated bilateral *in situ* non-cycled *ex vivo* perfusion of both hindlimbs. Ipsilateral and contralateral limbs were randomized for perfusion with either the UW perfusate with/without oxygen supplementation (control), or with the UW perfusate supplemented with the ATPv with/without oxygen supplementation (experimental). ATPv is an energy delivery vehicle capable of delivering ATP directly into the cytosol of the cells making up the composite tissue of the hindlimb. Both solutions were maintained at 4°C during preparation and perfusion. In situ perfusions with both solutions were delivered simultaneously from an infusion pump at a rate of 12 ml/min for a total wash-out- period of 25 min. Following this, the hindlimbs were surgically removed, labelled and placed in sterile bags for simple static cold storage over 12, 16 or 24 hours. At the end of each of designated three storage times, skin, soleus, extensor digitorum longus and tibialis anterior muscle samples were harvested from the control and experimental hindlimbs, and processed as required for the following measurements: 1) Limb and skin appearance; 2) Nitro blue tetrazolium chloride staining; 3) Tissue histology; 4) Wet-to-dry weight ratio; 5) Tissue extract studies of protein and small molecule biomarkers of oxidative stress (ELISA); 6) Early cytokine signature profiles in tissue extracts (ELISA).

3.1 Findings

1.1.1 Hindlimb and skin appearance: Inspection of the hindlimb and skin visually for appearance provided little information about composite tissue viability. There was no difference in hindlimb and skin appearance between the paired control and the experimental hindlimbs after 12, 16 or 24h of static cold storage. However, the color of the distal hindlimb at the end of perfusion was a good index of successful cannulation of the common iliac and of an adequate crystalloid *ex vivo* perfusion of the hindlimb. Upon adequate hindlimb perfusion, the distal digit of the hindlimb, which is not covered by skin changes to a whitish color suggesting complete flush out of the blood. This is further confirmed by the clear appearance of the perfusate recovered at the venous end and by the absence of red blood cells in the microvasculature in the histology sections.

1.1.2 Nitro blue tetrazolium chloride (NBT) staining: This is one of the measurements that were compromised by the hypothermic perfusion and the subsequent extended static cold storage of the hindlimbs. Specimen preparation for NBT staining requires the use of snap frozen muscle samples essentially in isopentane to preserve the nucleotide components of the nicotinamide adenine dinucleotide (NADH) enzyme from degradation. As our protocol required extended periods of hindlimb cold storage after ex vivo perfusion, the NBT staining proved difficult to achieve in our muscle sections, requiring both positive and negative controls. Because of these technical limitations, we decided to measure the activity of Succinate dehydrogenase (SDH) in muscle tissue lysates using commercial colorimetric assay kit (ab228560, abcam, USA). We performed the test in muscle tissue homogenized in 100 µL of SDH Assay Buffer and normalized the protein concentration in all samples as recommended by the manufacturer. SDH activity in the sample was determined from standard curve products generated with absorbance at 600 nm. The SDH enzyme is present in the inner mitochondrial membrane, where it exerts dual function in the citric acid cycle and the electron transport chain (just like NADH).

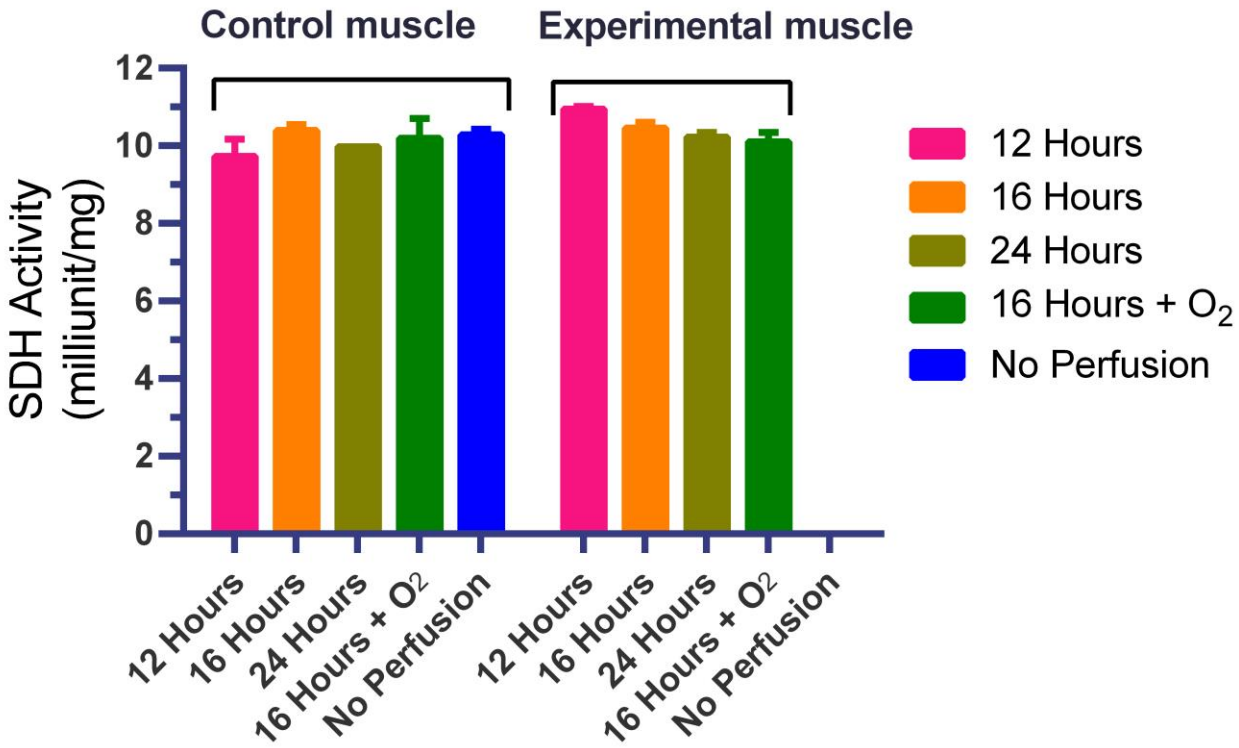

Figure 1: SDH activity in skeletal muscle after ipsilateral ex vivo perfusion (UW, control) or contralateral perfusion (UW + ATPv, experimental). One unit of SDH is the amount of enzyme that generates 1.0 µmole of DCIP per minute at pH 7.2 at 25 °C (Manufacturer). As seen in figure 1, SDH activity remained equally maintained in all muscle samples harvested after 12, 16 or 24 hours of static cold storage. Similar SDH activity was measured in soleus, extensor digitorum longus and tibialis anterior muscles regardless of the perfusate type or time of harvest. Therefore, the SDH activity reported in figure 1, represented the lumped SDH activity in all three muscle types. This data suggest that some level of tissue viability was preserved after ex vivo perfusion and subsequent static cold storage up to 24 hours. The addition of O_2 to the perfusate exerted no effect on the SDH activity. This prompted the need for additional indices of tissue viability to separate the control from the experimental.

1.1.3 Total tissue water contents: Total tissue water contents was determined from the tissue wet and dry weights. Tissues were samples from the soleus, extensor digitorum longus and tibialis anterior muscles in addition to the skin after ex vivo perfusion and static cold storage for 12, 16 and 24 hours. Samples were immediately weighed to determine their wet weight before drying to constant weight at 64°C. The data is shown in Figure 2.

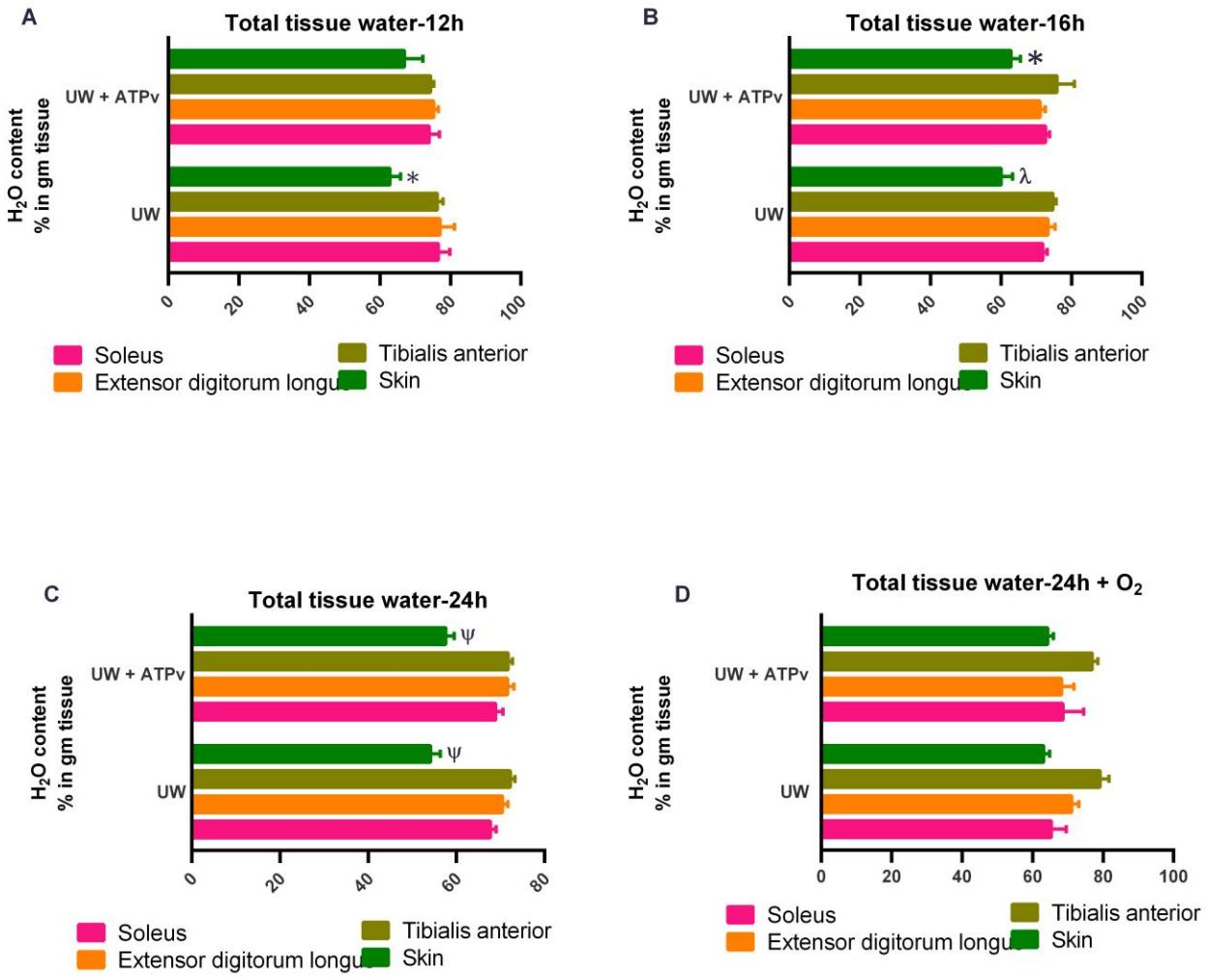

Figure 2. Total tissue water expressed as percentage in gram tissue weight. UW = University of Wisconsin solution (Control perfusion solution); UW + ATPv = Energy (ATPv) enhanced UW for ex vivo perfusion of the experimental hindlimb. * p = 0.0073 vs. soleus, extensor digitorum longus and tibialis anterior muscles by One-way Analysis of Variance and Tukey post-test corrected for

multiple comparison. # p = 0.037 vs. tibialis anterior by One-way Analysis of Variance and Tukey post-test corrected for multiple comparison; and § p = 0.0001 vs. soleus, extensor digitorum longus and tibialis anterior muscles by One-way Analysis of Variance and Tukey post-test corrected for multiple comparison.

1.1.4 Cytokine profile signatures in tissue lysates: This measurement was integral to our multitude of measurements that define the tissue viability index. Soleus, extensor digitorum longus and tibialis anterior muscle tissue samples were allocated from paired hindlimbs subjected to in situ *ex vivo* hypothermic perfusion with either the UW solution (control) or an energy enhanced (UW + ATPv) solution (experimental). Control and experimental hindlimbs were then preserved in static cold storage for either 12, 16 or 24 hours of cold ischemia times before the muscle tissue samples were harvested for cytokine profile signatures. To prepare for the measurement, we mixed each 1 mL of RIPA buffer (1x) with 10 µl of Sodium Orthovanadate (Na_3OV_4), 10 µl Sodium Fluoride (NaF), and protease inhibitor cocktail (1:99) for homogenization. We made a stock solution. Control and experimental muscle tissue samples were homogenized in 400 uL of the prepared solution using tissue homogenizers. The samples were centrifuged for 10 min at 4°C (13000 rpm). The centrifuged supernatants were transferred to properly labeled tubes stored at - 80°C ready for bicinchoninic acid assay (BCA) quantification of total protein and mRNA isolation. We used the BioTek Synergy HTX Multimode Microplate Reader at a 562 wavelength to determine total proteins in the tissue lysates. Initially, we considered to use the RT-PCR method to determine the cytokine signature profile as this method is the most commonly used for quantifying signatures of low-level transcripts such as cytokine and cytokine receptor mRNAs, particularly in small samples. We conducted a pilot study in randomly selected samples from the three cold ischemia times. In all samples, the mRNA was completely degraded during the extended cold tissue preservation times. Alternatively, we attempted to measure selected cytokine and chemokine proteins in randomly selected soleus tissue lysates using the Luminex multiplex technology (Luminex Magpix instrument/reader for sample acquisition and Luminex xPonent software for data analysis). As depicted in Table 1, the results from this pilot study confirmed the deleterious effects of extended static tissue cold storage on muscle tissue cytokine and chemokine proteins. These results were not surprising for several reasons: 1) isolated ex vivo perfusion with the UW crystalloid solution essentially flushes out major cytokine-producing immune cells from the vasculature of the hindlimb; 2) cytokine generation in response to an immune challenge is time dependent as largely influenced by immune modulators like IL-10. It is concluded that cytokine profiling is not a good index of composite tissue viability particularly after hypothermic tissue preservation protocols. However, this does not negate the critical cytokine role in the immune response that is associated with the reestablished blood flow upon allotransplantation.

	Soleus muscle		IL-1a pg/ml	IL-4 pg/ml	IL-1b pg/ml	IL-2 pg/ml	IL-6 pg/ml	IL-13 pg/ml	IL-10 pg/ml	IL-12 pg/ml	INF-ɣ pg/ml	IL-5 pg/ml	IL-17α pg/ml	IL-18 pg/ml	VEGF pg/ml	MIP-2 pg/ml	TNF-α pg/ml
16 hours	30-1 UW+ATPv 32-1 UW+ATPv 28-1 UW+ATPv	**Mean**	18.9	1332.0	25.8	11.6	201.1	30.5	194.9	59.7	3275.7	548.4	159.7	154.3	2829.3	82.2	5.7
		SD	14.4	1717.0	15.5	13.9	61.2	35.0	223.0	86.3	3786.8	668.1	254.3	87.3	1050.0	109.6	5.8
	30-1 UW 32-1 UW 28-1 UW	**Mean**	29.0	631.5	13.9	11.6	151.1	26.2	152.2	59.7	4177.3	166.5	158.2	376.1	3424.3	82.2	5.7
		SD	29.0	435.8	7.9	13.9	87.8	38.1	191.9	86.3	6413.5	112.3	255.6	384.8	3527.3	109.6	5.8
24 hours	20-1 UW+ATPv 26-1 UW+ATPv 19-1 UW+ATPv	**Mean**	5.2	118.6	4.9	4.2	63.6	26.2	16.3	17.2	826.3	206.1	4.2	91.5	474.6	30.4	2.4
		SD	1.6	115.2	4.5	1.1	12.6	5.6	3.3	12.7	609.4	286.2	2.1	102.9	593.7	13.1	0.1
	20-2 UW 26-2 UW 19-2 UW	**Mean**	31.4	733.5	19.1	11.6	161.1	26.2	136.4	159.3	2865.6	511.4	157.6	483.7	2944.3	82.2	5.7
		SD	22.3	617.4	17.9	13.9	94.5	38.1	161.9	86.3	4141.6	560.0	256.0	530.9	1843.6	109.6	5.8

Table 1. Multiplex ELISA Summary Report on selected cytokine proteins in soleus muscle lysates**.** UW = University of Wisconsin solution; ATPv = Energy (ATP) delivery vehicle; 16 and 24 hours designate the cold ischemia times after bilateral in situ ex vivo of the hindlimbs.

1.1.5 Tissue histology: We examined tissue histology sections (H&E stain) by light microscopy as integral to our multitude of measurements that define the tissue viability index. Skin and soleus, extensor digitorum longus and tibialis anterior muscle tissue samples were allocated from paired hindlimbs subjected to in situ ex vivo hypothermic perfusion with either the UW solution (control) or an energy enhanced (UW + ATPv) solution (experimental). Control and experimental Hindlimbs were then preserved in static cold storage for either 12, 16 or 24 hours of cold ischemia times before the skin and muscle tissue samples were sectioned for histology examination. Tissue biopsy studies are commonly used to assess viability of allografts. This provides information that are dependent on the site of the biopsy and the tissue type being biopsied. Beyond the structural integrity of the tissue, biopsy studies do not provide direct information about the functional integrity, and hence, viability of the composite tissue allografts. The major findings from our histology studies were as follows: 1) Tissue histology after 12, 16 or 24h of cold ischemia times, was not a sensitive method to detect distinct histologic differences between the three cold ischemia times within either control or experimental tissue sections; 2) Among the composite tissue types making up the hindlimb, the skin was the most tolerant to the cold ischemia of static cold storage, whereas, the vascular endothelium was the most sensitive; 3) A single noncyclic ex vivo perfusion of the hindlimb with an energy enhanced perfusate (UW + ATPv) protected the vascular endothelium from the damage of extended cold ischemia times; 4) Addition of O_2 to the energy enhanced perfusate did not exert additional protective benefits; and 5) Myocyte's nuclear density was the most valuable tissue histology parameter to reflect the effect of pathology and/or intervention.

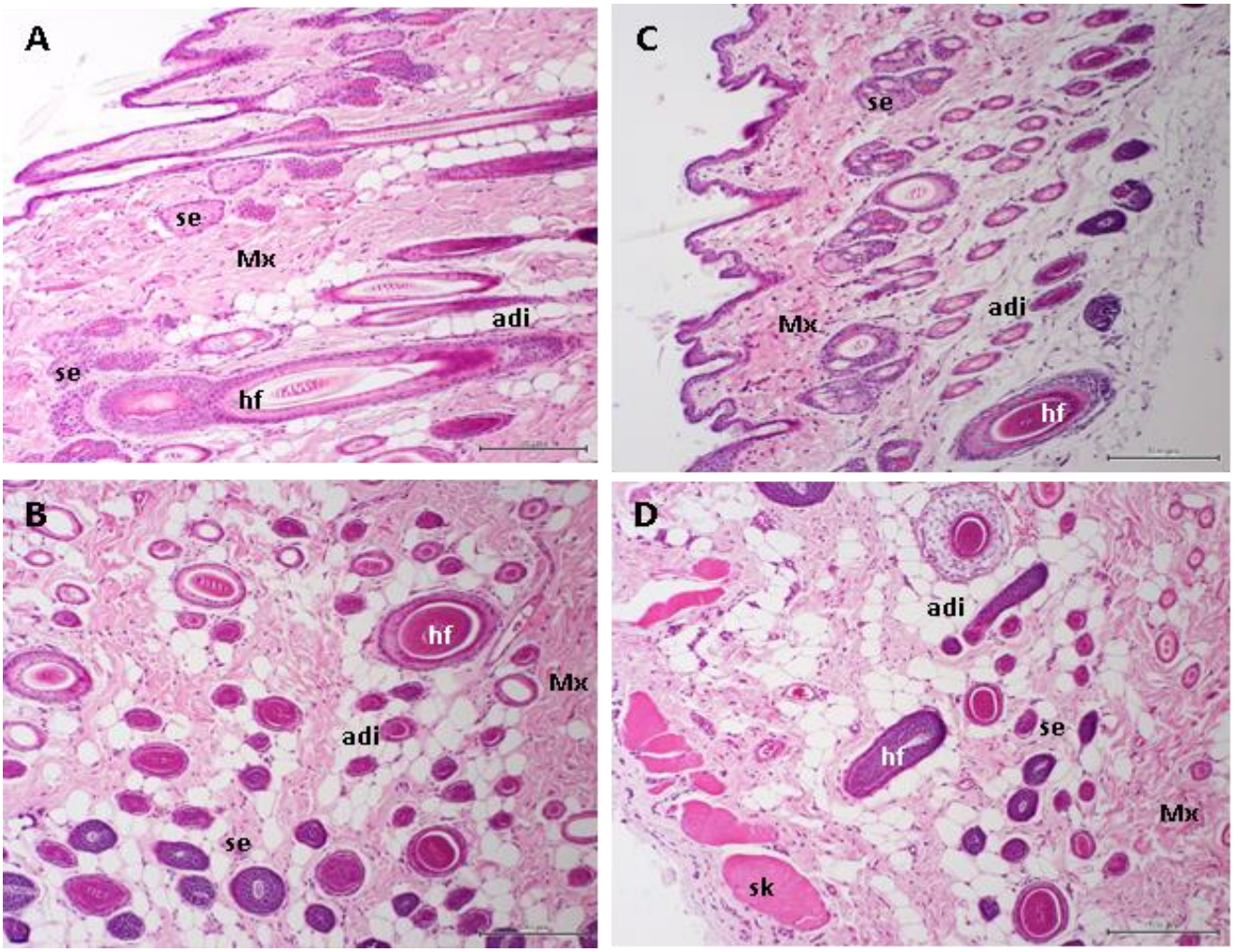

Figure 3. Light-microscopy photomicrographs of skin sections (H & E Stain) of a control hindlimb (A & B) subjected to ex vivo perfusion with the University of Wisconsin (UW) solution; and the paired experimental contralateral hindlimb (C & D) perfused with the UW solution plus ATPv. All skin sections were processed for histopathology after 24h of cold storage (4°C). Bar = 50 µm. adi = Adipocytes; seb = Sebaceous gland; hf = Hair follicle; sk = skeletal muscle; Mx = matrix of predominantly collagen and fibroblast. There were no definitive morphometric differences between the control and experimental skin sections.

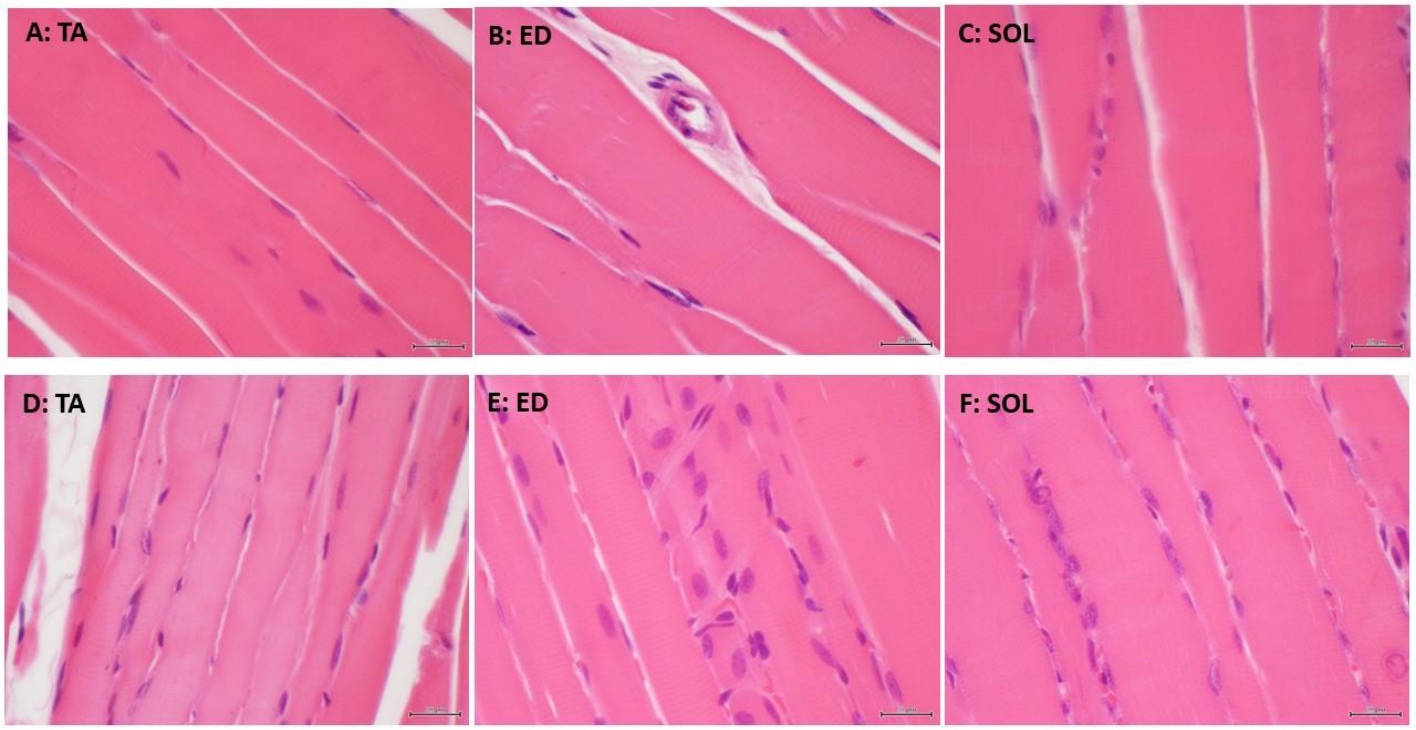

Figure 4. Light-microscopy photomicrographs of the tibialis anterior (TA), extensor digitorum longus (ED) and Soleus (SOL) muscle sections (H & E Stain) from a control hindlimb (A, B and C) that was subjected to ex vivo perfusion with the University of Wisconsin (UW) solution; and the paired experimental hindlimb (D, E and F) perfused with the UW solution plus ATPv. All muscle sections were processed for histology after ex vivo perfusion and subsequent 24h of static cold storage (4°C). Bar = 50 µm. As compared with the experimental muscle sections, the Control muscle sections (A,B and C) relative to the experimental muscle sections (D, E and F), show definitive decrease in the number of myocyte nuclei suggesting early myocyte necrosis. In addition, the experimental muscle section in D, E and F show numerous pale cytoplasmic satellite cells (regenerative myocytes). Both the control and the experimental muscles maintained the normal pattern of longitudinally arranged parallel muscle fibers.

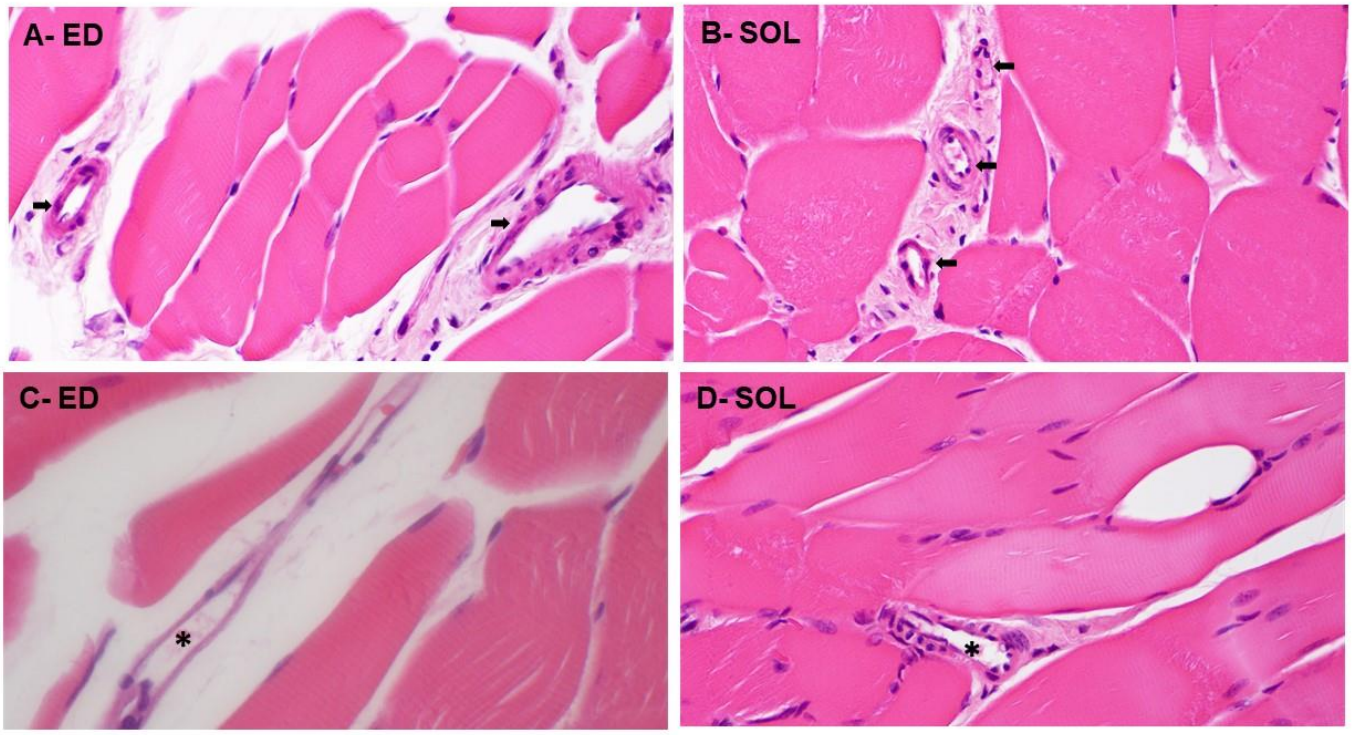

Figure 5. Light-microscopy photomicrographs of the extensor digitorum longus (ED) and Soleus (SOL) transverse muscle sections (H & E Stain) from a control hindlimb (A, B) that was subjected to ex vivo perfusion with the University of Wisconsin (UW) solution, and the experimental contralateral hindlimb (C, D) perfused with the UW solution plus ATPv. All muscle sections were processed for histology after ex vivo perfusion and subsequent 24h of cold storage (4°C). APTv = energy (ATP) delivery vehicle. Bar = 50 µm. The control ED and SOL muscle sections show thick-walled blood vessels with variable damage to the vascular endothelium (arrows). The experimental ED and SOL muscle sections show thin-walled venules (C-ED) and a blood vessel (D-SOL) with intact vascular endothelium relative to the control muscle sections.

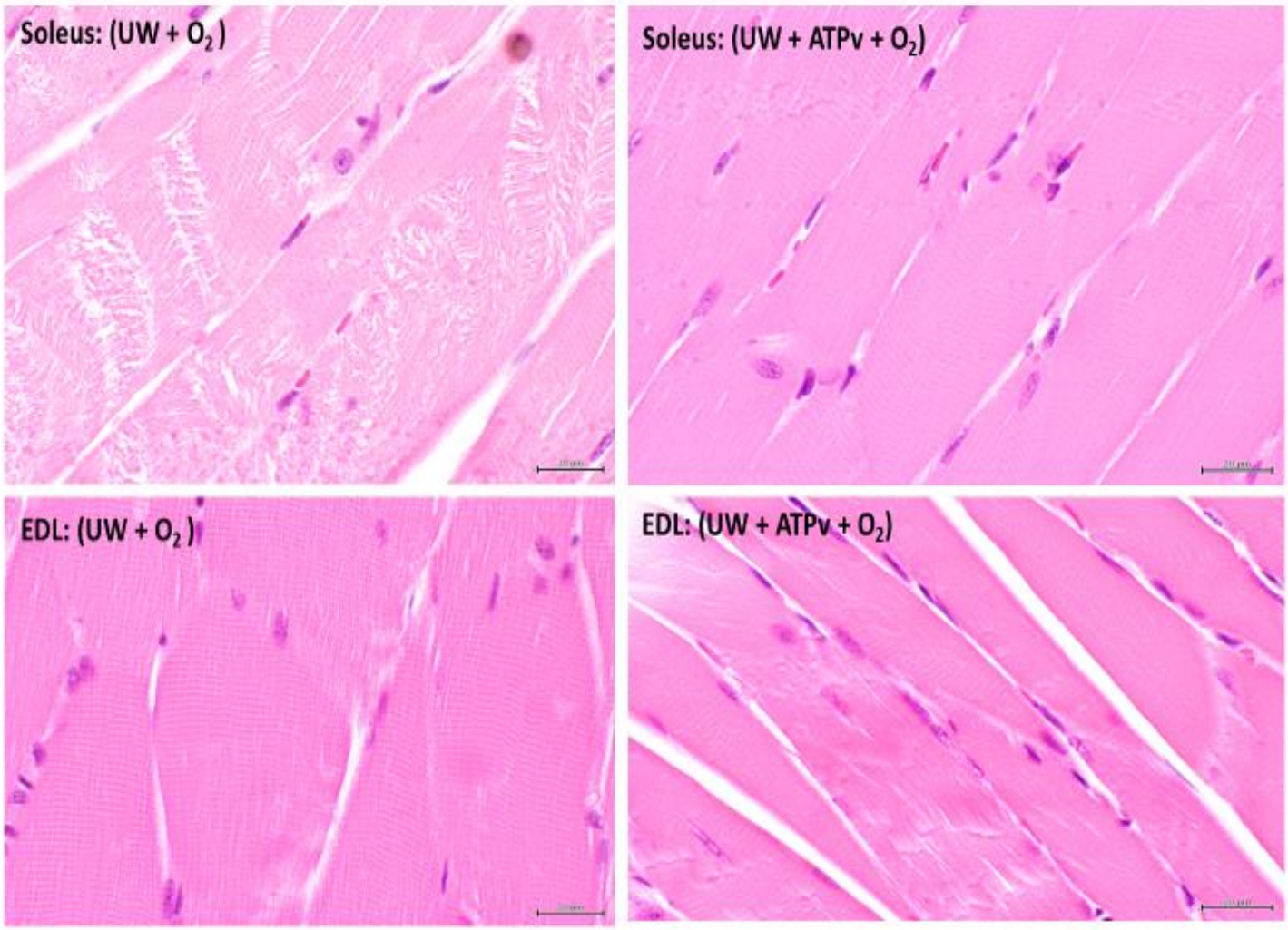

Figure 6: Effects of the addition of O_2 to the *ex vivo* perfusion solutions on muscle histopathology: Photomicrographs are thin sections (H & E Stain) of the soleus and the extensor digitorum longus (EDL) muscles**.** UW = University of Wisconsin solution; ATPv = energy (ATP) delivery vehicle. All muscles were processed for histopathology after 24h of static cold storage (4°C). Bar = 50 µm. As seen in the micrographs, the addition of O_2 to the *ex vivo* perfusion solution did not improve muscle tissue tolerance to static cold storage. All sections show definitive decrease in the number of nuclei suggesting early myocyte necrosis and areas of myocyte damage and degeneration are seen in all sections. The transverse striations of the soleus muscle fiber were totally lost with wider myocyte damage in the UW-perfused hindlimb. In the presence of supernormal O_2 saturation in the perfusate, ATPv exerted partial myocyte protective effects after ex vivo perfusion and subsequent 24h of cold storage (4°C).

Myocyte nucleus density: This was predefined as the number of myocyte nuclei per 40X microscopic field. Tibialis anterior, extensor digitalis longus and soleus muscles from a control hindlimb (ex vivo perfused with the UW solution), or an experimental hindlimb (ex vivo perfused with the UW + ATPv) were examined. A total of 3276 nuclei were counted in 169 fields of the control muscles in contrast to 3595 counted in 126 fields of the experimental muscles. This yielded 19 nuclei/field and 29 nuclei/field for the control and experimental muscles, respectively. The addition of O_2 to the control and experimental perfusates during the ex vivo perfusion yielded only 16 nuclei/field (total of 721 nuclei in 46 fields) of control muscles versus 22 nuclei/field (total of 472 nuclei in 21 fields) of experimental muscles. This data show that the addition of O_2 to the ex vivo crystalloid perfusion solution, which lacks an O_2 carrier exacerbates the myocyte's cold ischemia damage. In naïve anesthetized animals, a total of 3667 nuclei were counted in 143 fields, whereas 2727 nuclei were counted in 130 fields of the three muscle types from animals subjected to 3h of bilateral absolute hindlimb ischemia induced by aortic clamping, followed by 3 hours of reperfusion. This yielded 26 nuclei/field and 21 nuclei/field in muscles from naïve and ischemia/reperfusion animals, respectively.

ALTERNATIVE APPROACH TO REDEFINE ALLOGRAFT VIABILITY

Conservation of viability and functionality of the vascularized composite allograft (VCA), is critical to graft selection for allotransplantation. Current VCA conservation strategies are exclusive to static cold storage or extracorporeal hypothermic protocols. During the past decade, many optimizations to the extracorporeal perfusion protocols have been developed to improve viability, integrity and functionality of the VCA allografts. These adjustments included modifications of physical parameters like temperature and perfusion pressure/flow and ranged from continuous machine perfusion, to perfusion with blood or blood substitutes. Although these conservation strategies were intended to increase VCA tolerance to cold ischemia and protect against cell damage, their ability to create a positive cellular cytosolic energy balance to maintain VCA viability was not documented. As our energy enhanced ex vivo perfusion with ATPv directly replenishes the depleted cellular cytosolic energy stores, its impact on VCA viability must be elicited and evaluated at the subcellular and molecular levels. This rationale was supported by our data that demonstrated degradation of nucleotides and other protein ligands upon prolonged static cold storage. Such degradations compromised the potential use of ELISA or RT-PCR for detection of VCA molecular signatures as indicis of tissue viability. Therefore, we explored an alternative analytical approach that linked muscle proteome to subcellular structural changes. To define this subcellular structure-function relationship, we characterized the proteome of the soleus muscle and imaged thin sections of the muscle with transmission electron microscopy (TEM). Briefly, paired control and experimental soleus muscles from 3 animals were harvested at 24h of static cold storage after initial ex vivo non-cyclic hypothermic perfusion with the UW solution (control) or the UW + ATPv (experimental). To process the tissue for quantitative proteomics, the muscle samples were homogenized, and the total protein in the tissue lysate was determined by the BCA method. We used the BioTek Synergy HTX Multimode Microplate Reader at a 562 wavelength to determine total proteins in the tissue lysates. The data on total protein in the tissue samples are depicted in figure 7.

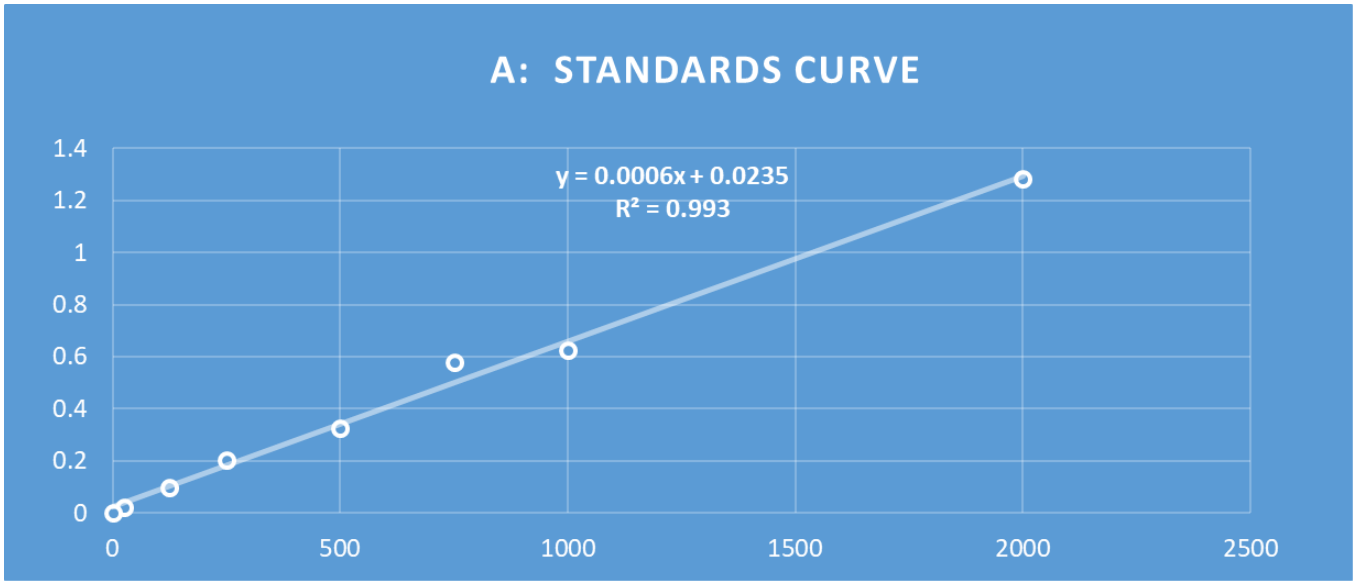

B: Total protein content

Sample ID	Samples: Abs (562)	Dilution c[µg/mL]	Actual c[µg/mL]
24-1 (UW, Control)	1.271	2079	41583.33333
24-2 (UW + ATPv, Experimental)	1.298	2123	42466.66667
25-1 (UW + ATPv, Experimental)	1.284	2101	42025
25-2 (UW, Control)	1.291	2112	42245.83333
26-1 (UW + ATPv, Experimental)	1.288	2107	42135.41667
26-2 (UW, Control)	1.289	2110	42190.625

Figure 7. BCA quantification of total protein in soleus muscle tissue lysates. UW = University of Wisconsin solution; ATPv = Energy (ATP) delivery vehicle; Abs = absorbance at a 562 wavelength.

Muscle proteome: Quantitative proteomics were conducted at the core facility of the University of Arizona. This was done according to the validated protocol depicted in figure 8. To prepare the soleus tissue lysates for quantification proteomics, 100 µg of homogenized muscle tissue lysate were separated on a 10% SDS-PAGE gel and stained with Bio-Safe Coomassie G-250 Stain. Each lane of the SDS-PAGE gel was cut into seven slices and subjected to trypsin digestion according to protocol. The resulting peptides were purified by C18-based desalting exactly as previously described by our validated protocol. The eluates were combined and dried completely by vacuum centrifugation and 6 µl of 0.1% FA (v/v) was added followed by sonication for 2 min. 2.5 µl of the final sample was then analyzed by mass spectrometry.

Mass spectrometry and database search: HPLC-ESI-MS/MS was performed in positive ion mode on a Thermo Scientific Orbitrap Fusion Lumos tribrid mass spectrometer fitted with an EASY-Spray Source (Thermo Scientific, San Jose, CA). NanoLC was performed exactly as determined by our validated protocol. Tandem mass spectra were extracted from Xcalibur 'RAW' files and charge states were assigned using the ProteoWizard 3.0 msConvert script using the default parameters. The fragment mass spectra were searched against the rattus SwissProt_2018_11 database (8068 entries) using Mascot (Matrix Science, London, UK; version 2.6.0) using the default probability cut-off score. The search variables that were used were: 10 ppm mass tolerance for precursor ion

masses and 0.5 Da for-product ion masses; digestion with trypsin; a maximum of two missed tryptic cleavages; variable modifications of oxidation of methionine and phosphorylation of serine, threonine, and tyrosine. Cross-correlation of Mascot search results with X! Tandem was accomplished with Scaffold (version Scaffold_4.8.7; Proteome Software, Portland, OR, USA). Probability assessment of peptide assignments and protein identifications were made using Scaffold. Only peptides with ≥ 95% probability were considered.

Label-free peptide/protein quantification and identification: Progenesis QI for proteomics software (version 2.4, Nonlinear Dynamics Ltd., Newcastle upon Tyne, UK) was used to perform ion-intensity based label-free quantification according to our protocol. Extracted ion abundance data was then further processed and visualized using the open-source software program designed for bioinformatics analysis of –omics data, Perseus according to protocol (figure 8).

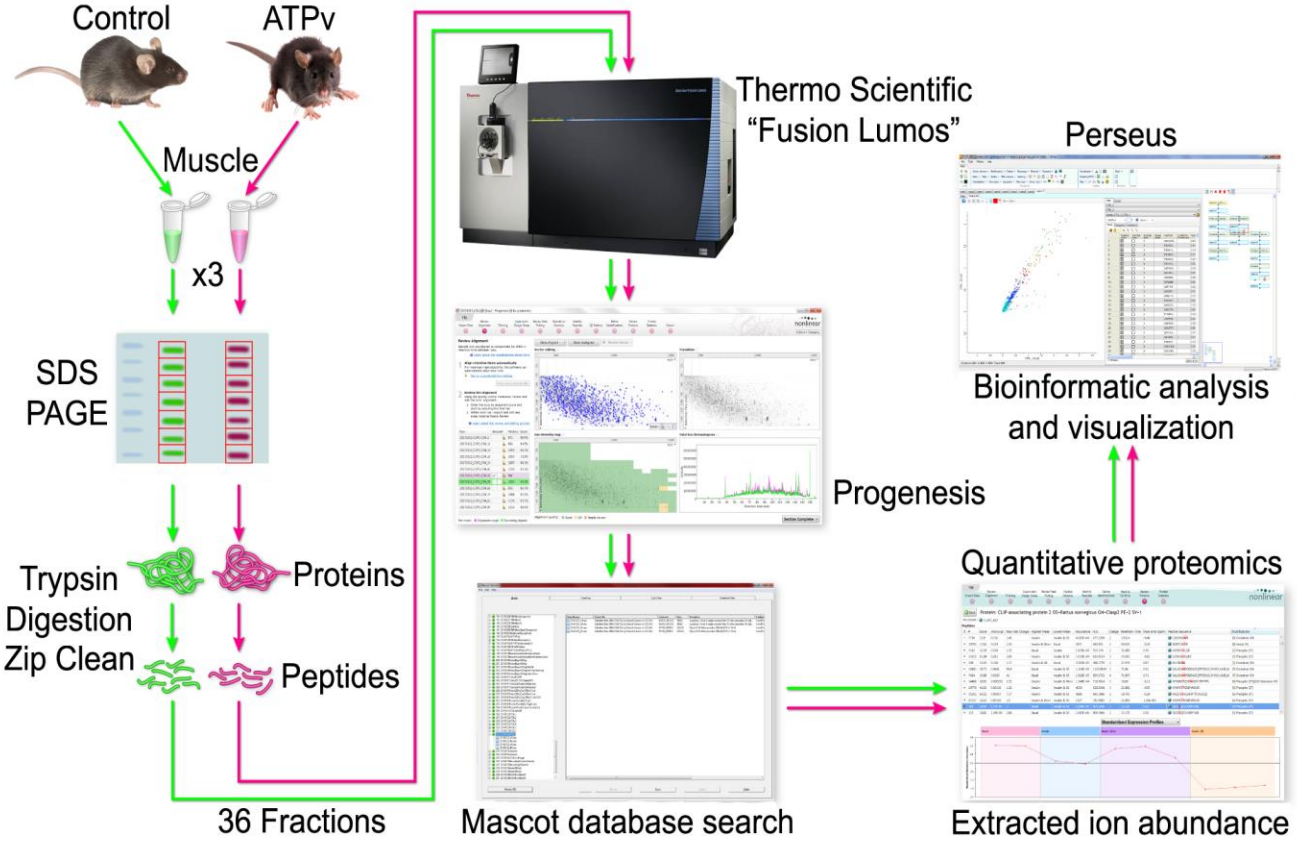

Figure 8. Experimental protocol for defining and characterizing the soleus muscle proteome. Control = ipsilateral hindlimb subjected to ex vivo hypothermic perfusion with the University of Wisconsin solution (UW); IPTv = the contralateral hindlimb that was subjected to ex vivo hypothermic perfusion with the experimental energy (ATP) enhanced University of Wisconsin solution (UW + ATPv); ATPv = energy delivery vehicle; SDS-PAGE = sodium dodecyl sulphate-polyacrylamide gel electrophoresis.

We performed quantitative proteomics comparing global protein expression changes between control versus experimental soleus muscle tissue as described and outlined in Figure 8 (n=3). 2185 total proteins were identified, of these 2120 (97%) were non-significantly affected whereas 65 (3%)

were significantly different between the two groups, with 43 proteins exhibiting an increase and 22 proteins exhibiting a decrease in the experimental muscle tissue as compared to controls (figure 9B). Unbiased principal component analysis of the 65 significantly affected proteins revealed that the protein expression differences of the individual biological samples within each group were consistent and no outliers were detected (figure 9A). Unbiased hierarchical clustering of the 65 significantly affected proteins confirmed that the expression patterns across the different individual biological samples cluster together accordingly as either control or experimental (figure 9A). A heat map and linked dendrogram of the hierarchical clustering results provide a visual representation of the clustered matrix and the associated profile plots further reveal consistency within groups of the corresponding protein expression patterns (figure 9B).

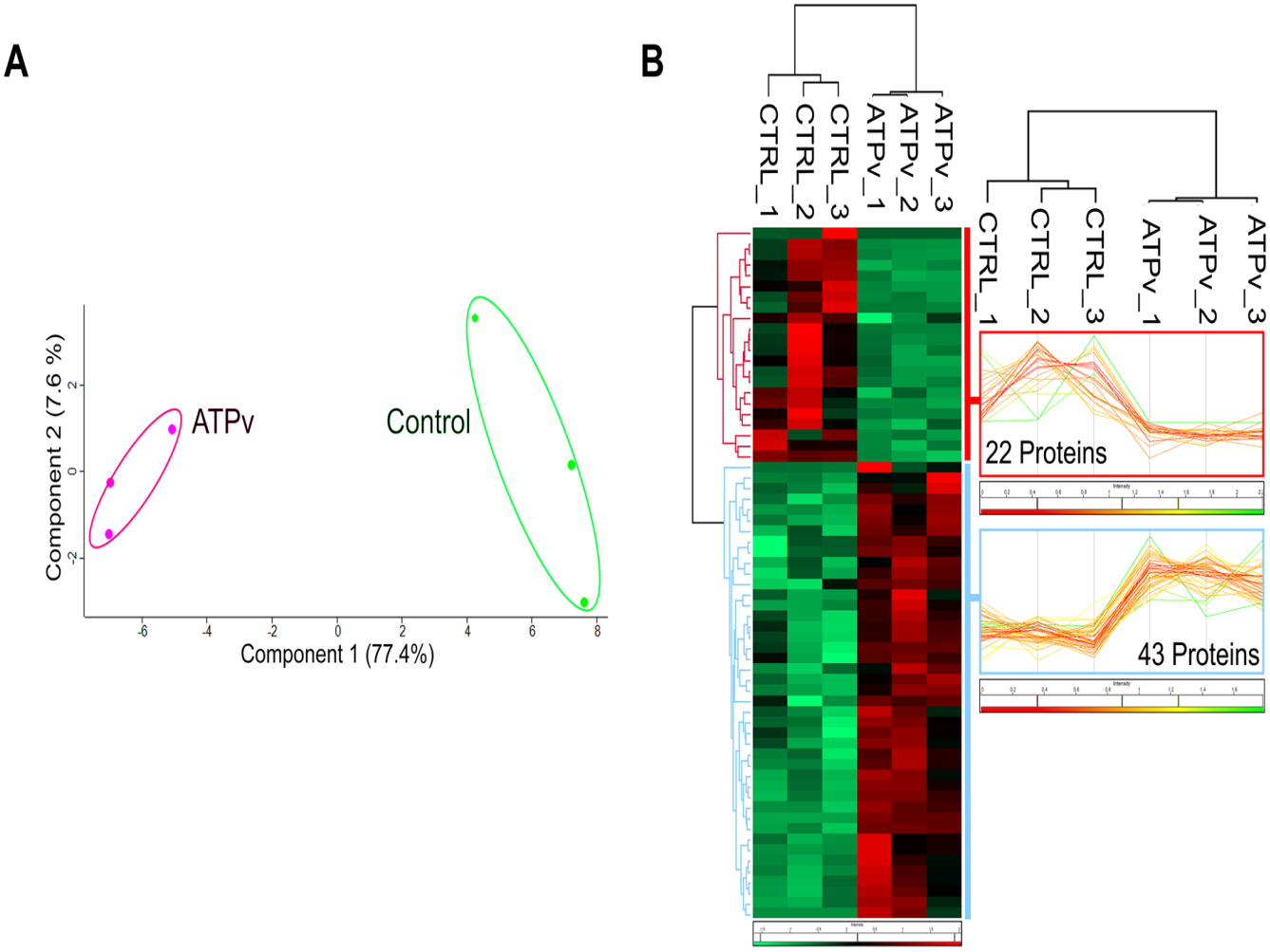

Figure 9. Principal component analysis of the 65 significantly affected proteins between the control (CTRL) and experimental (ATPv) soleus muscles, showing variability within between groups (A). Heat map and linked dendrogram of the hierarchical clustering results between the CTRL and ATPv soleus muscles (B). Control = ipsilateral hindlimb subjected to ex vivo hypothermic perfusion with the University of Wisconsin solution (UW); IPTv = the contralateral hindlimb that was subjected to ex vivo hypothermic perfusion with the experimental energy (ATP) enhanced University of Wisconsin solution (UW + ATPv); ATPv = energy delivery vehicle.

We also represented our data in a volcano plot (Figure 10), permitting an overall visualization of significance and fold-change. These results are supportive of consistent, reproducible, and distinct protein abundance differences in the experimental soleus muscle tissue as compared to controls.

The 65 significantly affected proteins were searched against the Database for Annotation, Visualization, and Integrated Discovery (DAVID) gene ontology classification system for statistically over- and under-represented in KEGG pathways and gene ontology (“GO”) tags among the genes in the Biological Processes, Cellular Component, and Molecular Function clusters. The 65 significantly affected proteins displayed significant enrichment across a multitude of GO clusters and KEGG pathways, which can now be used to develop hypotheses aimed at exploring mechanisms underlying the increased VCA tissue tolerance to extended cold ischemia times after cellular cytosolic energy (ATP) replenishments (figure 11).

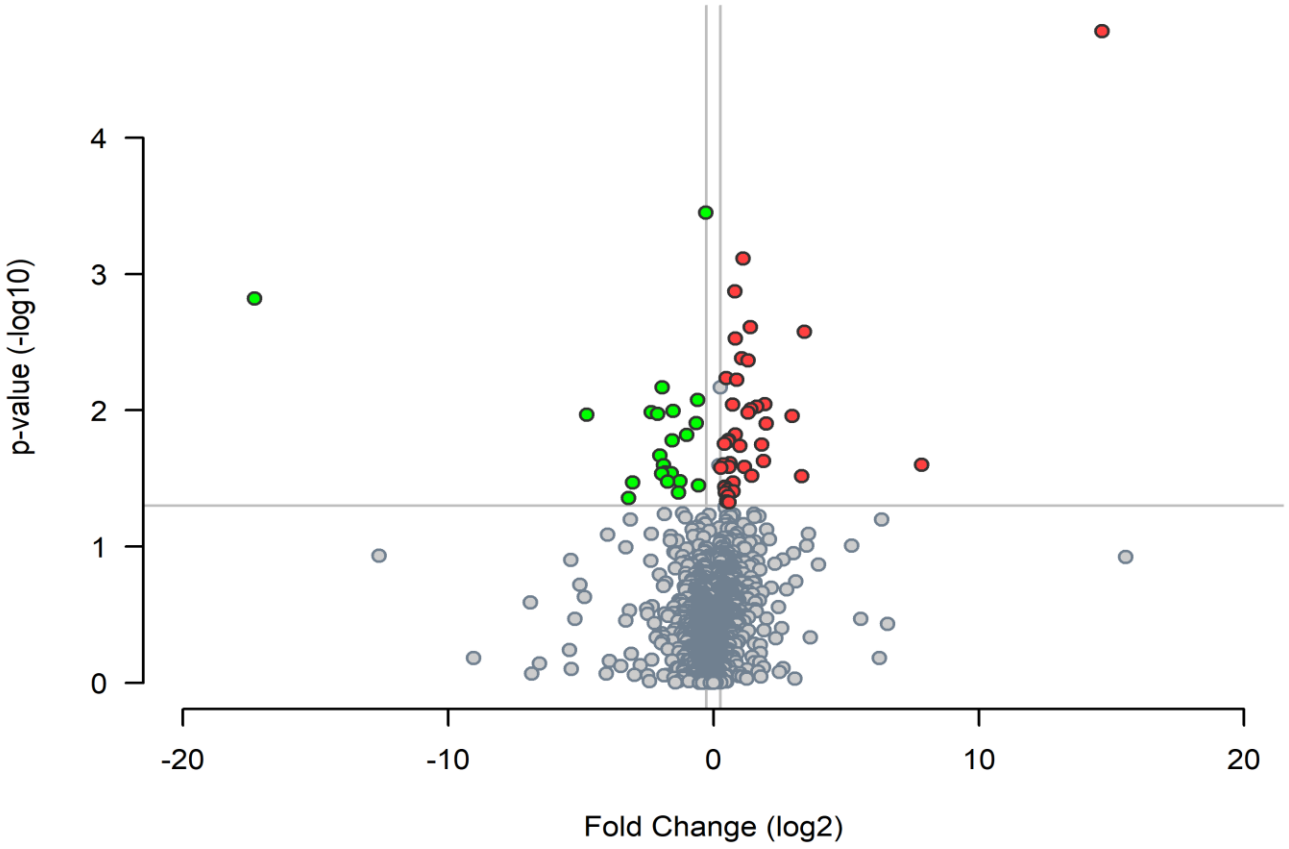

Figure 10. Volcano plot visualizing significance and fold-change in protein abundance between the control and experimental soleus muscles. The gray symbols below the horizontal line represent the 2120 proteins that were not changed between the control and experimental muscles. Above the horizontal line are the 65 proteins that either exhibited a significant increase (red symbols) or a decrease (green symbols) in the experimental as compared to the control soleus muscle.

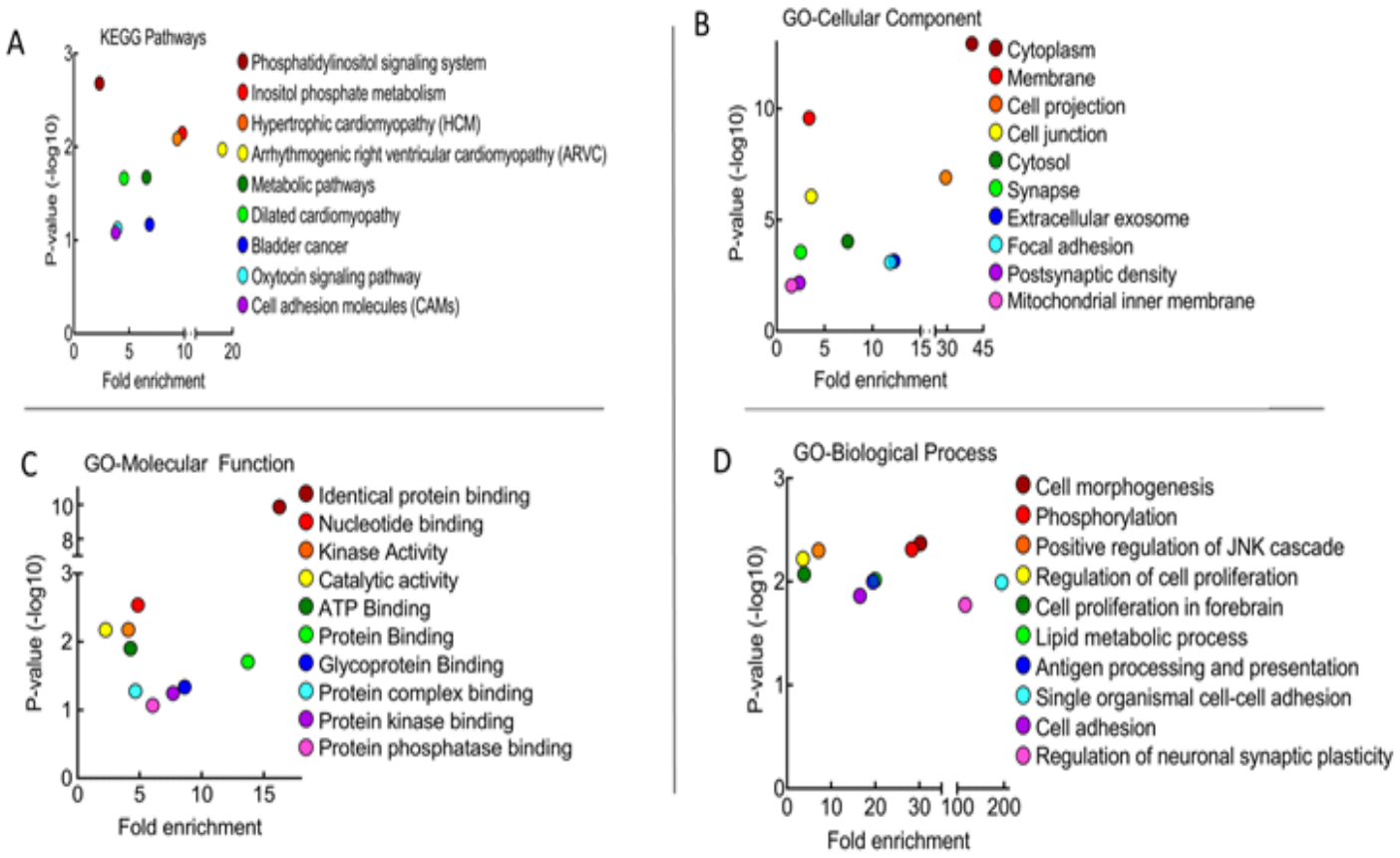

Figure 11. Functional interpretation of statistically significant over represented genes realized in the Kyoto Encyclopedia of Genes and Genomes (KEGG) systems category database for pathway maps of cellular and organismal function (A); and the gene ontology ("GO") tags for cellular component (B), molecular function (C) and biological process (D). Panel B showed >10 folds abundance of extracellular exosomes (GO:0070062) in the ATPv perfused soleus muscle lysates. These are extracellular exosomes that originate from the cellular endosomal compartment and contain various proteins and a cargo of mRNA and miRNA that are derived from their cell of origin. The presence of the extracellular exosomes in the peripheral blood and in urine make them ideal for use as biomarkers.

Transmission Electron Microscopy (TEM): To complement our quantitative proteomics with subcellular structural component measurements, we performed TEM to link subcellular functions to subcellular structural changes as an index of tissue viability. TEM was conducted on paired soleus, extensor digitorum longus and tibialis anterior muscles after simultaneous ipsilateral ex vivo perfusion with the UW solution (Control) and contralateral UW+ATPv energy-enhanced solution (Experimental). Both the Control and the experimental hindlimbs were preserved in static cold storage for 24h before the muscles were harvested for TEM. Representative TEM micrographs were shown in figures 12 – 15.

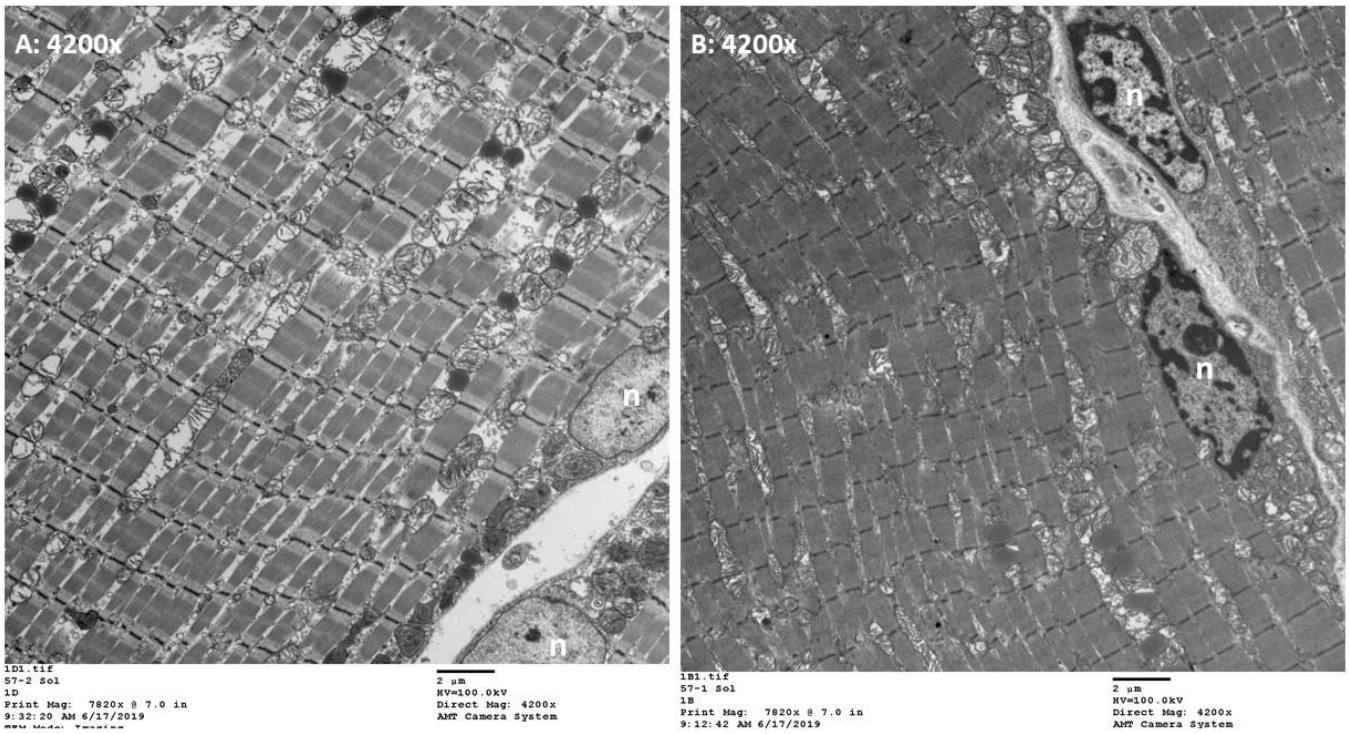

Figure 12. Transmission electron micrograph (TEM) of longitudinal sections through paired control (A) and experimental soleus muscles at 4200x. The striated banding-pattern of the muscle fibrils was maintained in both control and experimental sections. The fibrils run in parallel and between them runs sarcoplasmic reticulum and mitochondria that appeared proliferative in number and size in the control muscle section (A). Within each fibril were the sarcomeres separated by lines. Each contractile sarcomere has protein filaments of myosin and actin that functionally slide over each other, thereby causing the whole muscle to contract. The myofibrils appeared to have nuclei (n) with different morphometric attributes between the control and the experimental soleus muscles. Some areas of myofibrils damage were seen in the control soleus muscle.

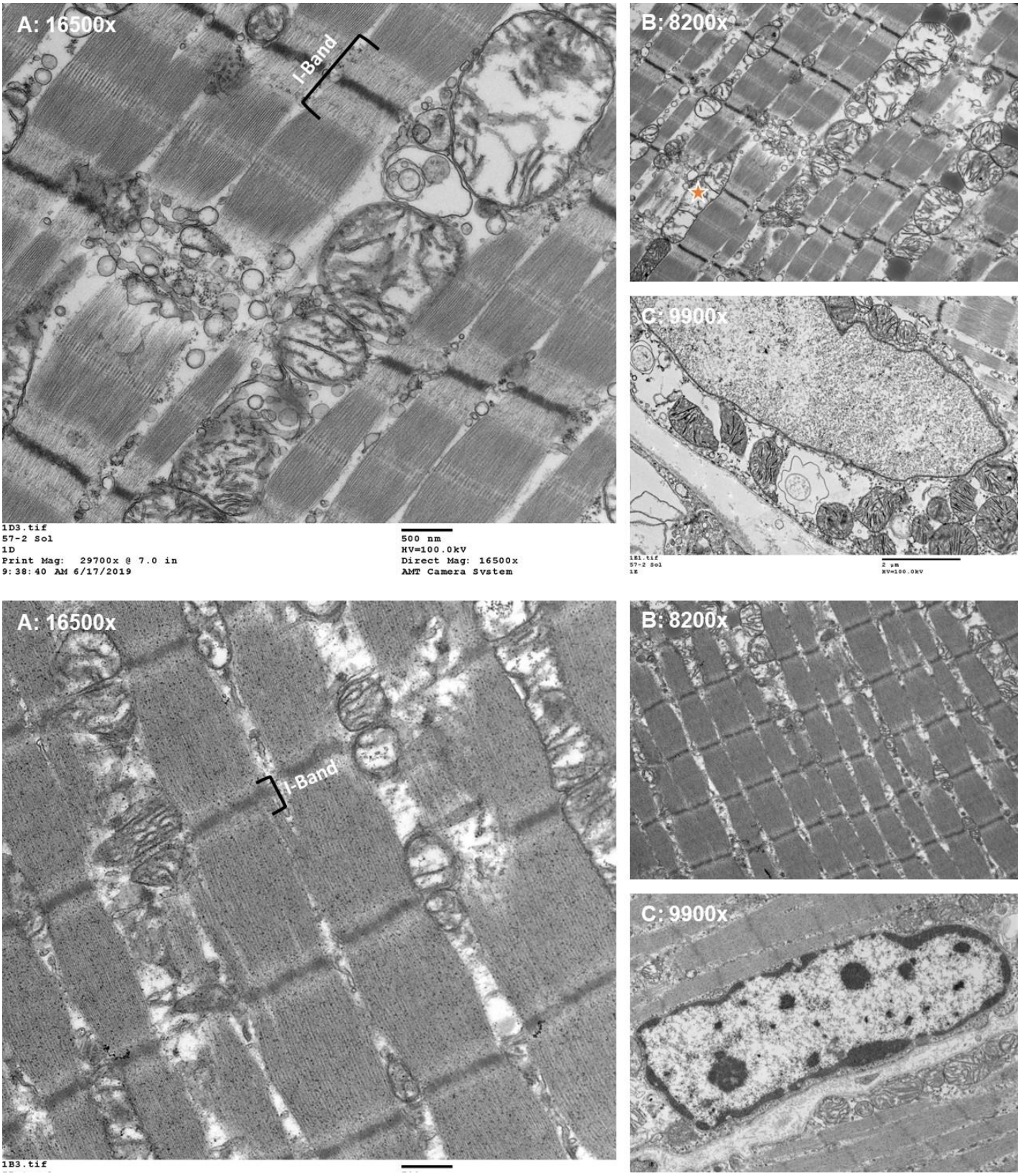

Figure 13. Transmission electron micrograph (TEM) of longitudinal sections through paired control (upper panel) and experimental (bottom panel) soleus muscles at different magnifications to highlight important morphometric structural and functional differences. The control muscle myofibrils (A: upper panel) showed distinct I-band (actin filaments) as compared with the experimental muscle (A: bottom panel, suggesting 25% contraction of the experimental myofibrils. Interfibrillar mitochondria of the control soleus muscle were proliferative in number and morphology including elongated string mitochondria (B: star symbol). The mitochondria beneath the sarcolemma

appeared of normal size and morphology in both the control and experimental soleus muscles (C). The double-layer mitochondrial membrane remained intact in both control and experimental muscles. The myocyte nucleus of the control soleus muscle showed diffuse and loosely arranged euchromatin (C: upper panel). The experimental soleus muscle showed dark and dense heterochromatin in close arrangement to the nuclear envelope. The nucleolus appeared as a very dark and dense rounded structure in the nucleoplasm (C: bottom panel).

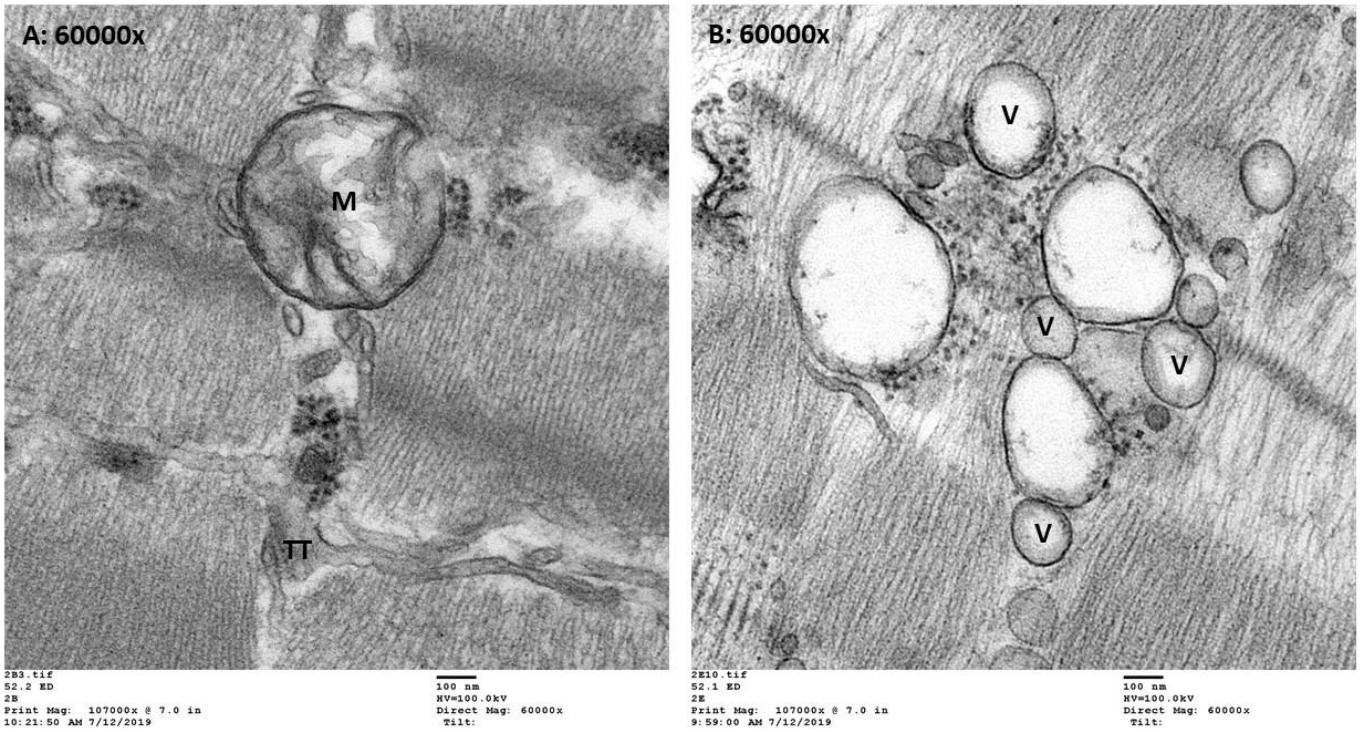

Figure 14. Transmission electron micrograph (TEM) of longitudinal sections through paired control (A) and experimental (B) extensor digitorum longus muscles. V = intercellular vesicle; M = mitochondrion; TT = transverse tubule. The contraction bands appeared uniformed in the control but diffused and disrupted in the experimental. The mitochondrion in the control section (A) showed cristae with partial loss of the external membrane.

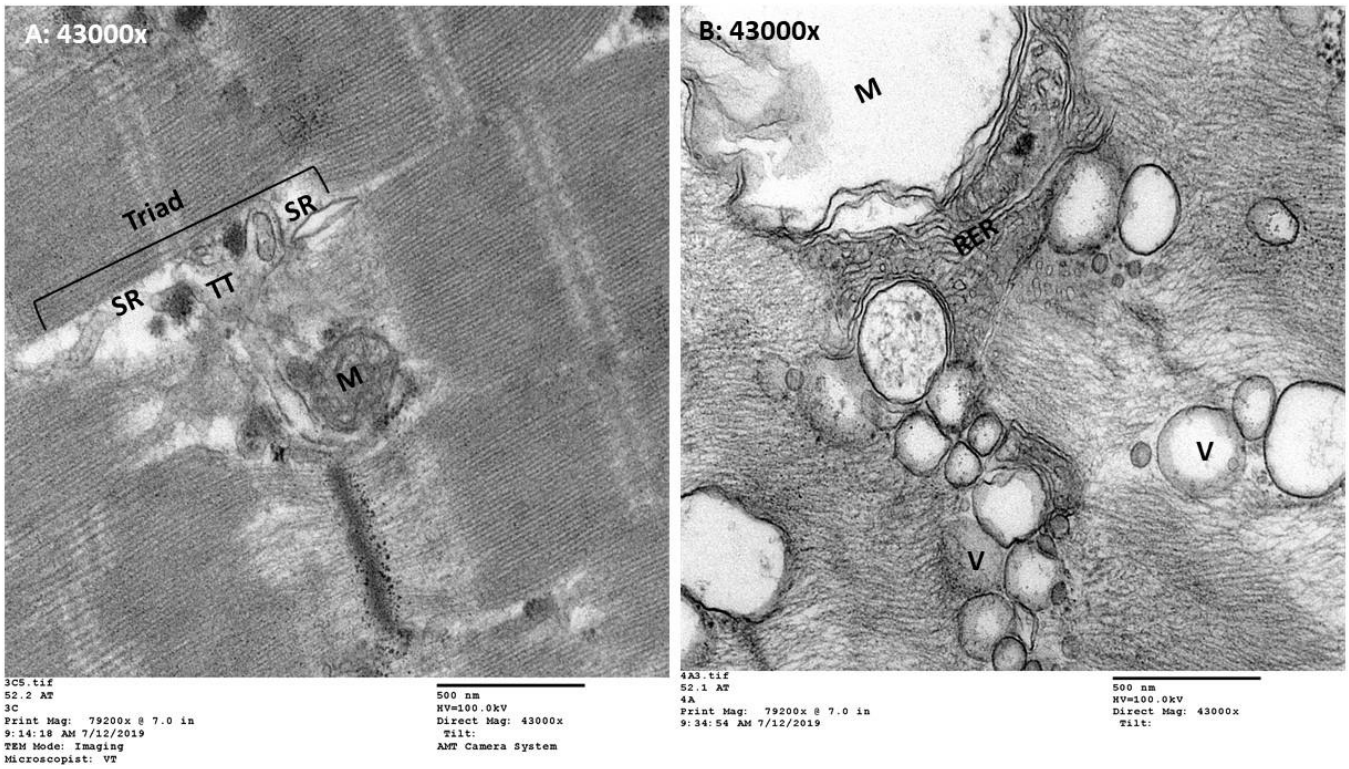

Figure 15. Transmission electron micrograph (TEM) of longitudinal sections through paired control (A) and experimental (B) Tibialis anterior muscles. V = intercellular vesicle; M = mitochondria; TT = transverse tubule. Triad = sarcoplasmic reticulum (SR) on either side of the TT. The contraction bands appeared uniformed in the control but diffused and disrupted in the experimental. The mitochondrion in the control section (A) showed cristae with loss of the external membrane; however, the experimental section showed a mitochondrion without any pattern of cristae but an intact bilayer membrane.

Summary of Findings: Current composite tissue conservation strategies were adopted from solid organ preservation techniques that varied between static cold storage and continuous hypothermic machine perfusion protocols. Unlike solid organs, the composite tissue allografts contain different tissue types with different metabolic demands. We used a rat model of isolated bilateral in situ non-cycled ex vivo perfusion of both hindlimbs. In this model, ipsilateral and contralateral hindlimbs were randomized for paired perfusion either with the UW perfusate with/without oxygen supplementation (control) or with the UW perfusate supplemented with ATPv with/without oxygen supplementation (experimental). We were able to provide a direct evidence that supported the following:

1) Energy enhanced (ATPv) ex vivo hypothermic perfusion, increases hindlimb composite tissue tolerance to extended cold ischemia times (12 – 24 hours) during static cold storage without significant vascular and muscle damage.
2) The protective effects of the energy enhanced (ATPv) ex vivo hypothermic perfusion system can be further enhanced by cyclic or continuous hypothermic machine perfusion to achieve a positive cellular cytosolic energy balance without the need for static cold storage.
3) Tolerance to cold ischemia is not equal between the tissue types of the hindlimb allograft. The vascular endothelium exhibits the least tolerance relative to the skeletal muscle and skin.
4) The addition of O_2 to the UW control or the ATPv enhanced experimental ex vivo perfusion solutions did not exert any incremental protective effects of composite tissue tolerance to 24h of cold ischemia time.

5) Supernormal O_2 concentrations dissolved in the ex vivo UW-perfusion solution produced remarkable myocyte damage characterized by decreased nuclear density after 24h of static tissue cold storage. This damage was alleviated but not completely prevented by the addition of ATPv to the ex vivo perfusion solution.
6) Extended static cold preservation completely degraded composite tissue RNA to the extent that RT-PCR or ELISA techniques for the detection of cytokine and chemokines signature profiles cannot be used. In addition, the initial perfusion with the crystalloid solution flushes out blood cellular elements, which are the major source for cytokines and chemokines. This critical conclusion suggested that other commonly used imaging techniques, such as immunohistochemistry and nitroblue-tetrazolium (NBT) techniques cannot be used to assess tissue viability particularly after extended static cold storage. These techniques are based on tissue localization of intermediaries within the metabolic pathways and therefore do not provide any indication to the prevailing allografts tissue function.

Opportunities and professional development: We provided research training to two students who participated in tissue homogenization, protein isolation and data entry. The students were also taught the basics of research methods and muscle physiology. One participant, a high school student was recruited from the Summer Institute on Medical Ignorance, which is a program sponsored by the College of Medicine of the University of Arizona. The second participant was a graduate student who was recruited as an NIH-Undergraduate Student Summer Research Program scholar. We also provided high level training on rodents' surgery including cannulation and microsurgical procedures to two research associates who conducted the experiments of this project.

Results dissemination: The data was partially presented locally at the Annual Research Day of the University of Arizona and at the Seminar of the Underserved Underrepresented Students at the University of Arizona. As required, we will present the completed project at the next Military Health System Symposium in 2020.

IMPACT

4.1. ***Impact on VCA Surgery:*** By increasing the composite tissue allograft tolerance to extended cold ischemia times, we removed a critical obstacle that for so long has limited the routine clinical use of this restorative allotransplantation surgery. Although we performed a single noncyclic ex vivo perfusion with the ATPv enhanced solution, viability of the composite tissue can be better maintained and sustained by cyclic or continuous ATPv machine perfusion without the need for static cold storage. The cyclic or continuous delivery of ATP to the cytosol of the cell would create a positive ATP balance that support the energy-dependent cellular processes. This will be of greater importance when reviving the high-risk composite tissue allografts procured from the brain-dead donor. For this reason, it is imperative to devise strategies in the brain-dead management protocol to increase composite tissue tolerance to the warm ischemia time and decrease the systemic inflammation that is associated with brain death. Existing guidelines for donor management protocols are intended to maximize viability and function of the procured solid organs and to enhance the procurement rate of multiple organs from a single donor. These guidelines might not apply to the vascularized composite tissue allografts because of the following considerations: I) composite allografts contain different tissue types that differ in their tolerance to the ischemic hypoxia, hypoperfusion and metabolic demands; II) the redistribution of the cardiac output away from the skin and skeletal muscle negatively affects these major components of the composite tissue; III) lack of quality indicators for the composite tissue allografts; and IV) the inevitable need for extended composite tissue preservation by hypothermic extracorporeal protocols or simple static cold storage.
One strategy that has been shown to decrease the burden of brain death on solid organs in animals and in humans is the adjuvant therapy of direct peritoneal resuscitation (DPR). Adjuvant DPR

utilizes glucose-based clinical peritoneal dialysis intraperitoneally as integral with the brain-dead management protocol. This non-drug therapy rapidly enhances abdominal and distant organ blood flow and decreases circulatory inflammatory markers, edema as well as the need for vasopressors. Because of these qualities, DPR therapy is now an integral of the brain-dead management protocol in the State of Kentucky. As our results show, the integration of the evidence-based continuous cellular cytosolic ATP replenishment together with the DPR technique will create a new paradigm to enhance viability and availability standards for composite tissue allografts and solid organs alike.

4.2. ***Impact on health care cost:*** Complex injuries of the craniofacial region and amputations are associated with significant soft tissue, bone, nerve and skin losses. Treatment of these disfiguring injuries requires multistep reconstructive and plastic surgery procedures. Amputations are commonly masked with the use of cosmetic prothesis. These treatment options come with high health care and rehabilitation costs not to mention the psychological impact on the injured and the burdens on their care givers. If successful, partial or complete vascularized composite allotransplantation remains the definitive treatment that potentially can restore appearance, anatomy and function of the transplanted composite tissues at a remarkably lower health care cost.

CHANGES/PROBLEMS

The cold ischemia time during the extended static cold storage of the hindlimb invariably degraded the composite tissue nucleotides and nucleic acids and violated the optimal temperature required for tissue/cell enzyme activity. Applications that are based on nucleotides for detection like RT-PCR, on specific antibody conjugates like ELISA, or on specific antibodies binding to the antigens like immunohistochemistry are therefore unreliable tests for composite tissue viability particularly after extended cold storage of the composite tissue. Because of these limitations, we sought a better index to define tissue viability. ATPv delivers the high energy ATP molecules directly into the cytosol of cells. Therefore, the sequels of the ATP-enriched cytosol must be realized and elicited at the immediate subcellular microenvironment. For this reasoning, we exploited a possible link between subcellular structure-function relationship as a potential measurement index of hindlimb viability. The subcellular structural changes were determined by transmission electron microscopy (TEM), whereas the subcellular molecular functions were evaluated by quantitative proteomics. After ex vivo perfusion and subsequent 24h of hindlimb's cold ischemia, remarkable subcellular structural changes were noted much in accordance with the ex vivo perfusion solution.

In the UW-perfused control hindlimb, the subcellular structural changes were predominantly seen as proliferations in the mitochondrial shape and number. The spectrum of the mitochondrial ultrastructural abnormalities ranged from simple uniform swelling, string elongation, linearization or loss of cristae, matrix compartmentalization, donut-shaped matrix and partial loss of the external membrane. These mitochondrial ultrastructural defects are highly suggestive of mitochondrial dysfunction. In contrast, in the ATPv-perfused experimental hindlimb, mitochondrial shape and number were largely preserved, but proliferative intracellular vesiculation was noted particularly in the extensor digitorum longus and the tibialis anterior muscles. Intracellular vesicles varied in their size and in their encapsulated contents. They are known to perform cellular functions ranging from intracellular material trafficking, digestion and extracellular secretion suggesting active subcellular processes. More importantly, a 25% contraction was noted in the myofibril contractile proteins. Taken together with the quantitative proteomics, this new analytical approach although invasive and time consuming, it has a predictive value in assessing composite tissue viability after their extended cold storage. More studies are needed for the optimization of the ATPv delivery protocol to enable generalization of the results. For the clinical assessment of composite tissue allograft viability and function, further effort is required to identify tissue viability-specific biomarkers to facilitate the rapid selection of composite tissue for allotransplantation.

PRODUCTS

Nothing to report.

PARTICIPANTS & OTHER COLLABORATING ORGANIZATIONS

Name:	*El Rasheid Zakaria*
Project Role:	*PI*
Researcher Identifier (e.g. ORCID ID):	*0000-0003-3230-073X*
Nearest person month worked:	*11*
Contribution to Project:	*Obtained regulatory approvals, hired and trained staff. Experimental design, data interpretation, oversight of experiments. Reporting.*
Funding Support:	
Name:	*Bellal Joseph*
Project Role:	*Co-Investigator*
Researcher Identifier (e.g. ORCID ID):	
Nearest person month worked:	*2*
Contribution to Project:	*Data interpretation*
Funding Support:	
Name:	*Ibtehal Ahmed*
Project Role:	*Research Associate*
Researcher Identifier (e.g. ORCID ID):	
Nearest person month worked:	*3*
Contribution to Project:	*Performed experiments and harvested tissues for measurements of tissue water and histology.*
Funding Support:	
Name:	*Abdul Wali Yousufazi*
Project Role:	*Research Associate*
Researcher Identifier (e.g. ORCID ID):	
Nearest person month worked:	*6*
Contribution to Project:	*Performed experiments and harvested tissues for measurements of tissue water and histology. ELISA.*
Funding Support:	
Name:	*Chiu-Hsieh Hsu*
Project Role:	
Researcher Identifier (e.g. ORCID ID):	
Nearest person month worked:	*2*
Contribution to Project:	*Biostatical support and data analysis.*
Funding Support:	
Name:	*Anthony German Martinez*
Project Role:	*Volunteer*
Researcher Identifier (e.g. ORCID ID):	
Nearest person month worked:	*1.5*
Contribution to Project:	*Volunteer, performed tissue homogenization and protein extraction and data entry.*

Funding Support:	*University of Arizona*
Name:	*Viktoras Sangster-Biye*
Project Role:	*Volunteer*
Researcher Identifier (e.g. ORCID ID):	
Nearest person month worked:	*1*
Contribution to Project:	*Volunteer, performed tissue homogenization and protein extraction and data entry.*
Funding Support:	*University of Arizona*

SPECIAL REPORTING REQUIREMENTS

Updated quad chart submitted as attachment.

APPENDICES

Two manuscripts are being drafted for submission to the American Journal of Transplantation.